

Detection of differential gene expression in brown adipose tissue of hibernating arctic ground squirrels with mouse microarrays

Jun Yan, Adlai Burman, Calen Nichols, Linda Alila, Louise C. Showe, Michael K. Showe, Bert B. Boyer, Brian M. Barnes and Thomas G. Marr

Physiol. Genomics 25:346-353, 2006. First published Feb 7, 2006;
doi:10.1152/physiolgenomics.00260.2005

You might find this additional information useful...

Supplemental material for this article can be found at:

<http://physiolgenomics.physiology.org/cgi/content/full/00260.2005/DC1>

This article cites 32 articles, 19 of which you can access free at:

<http://physiolgenomics.physiology.org/cgi/content/full/25/2/346#BIBL>

Updated information and services including high-resolution figures, can be found at:

<http://physiolgenomics.physiology.org/cgi/content/full/25/2/346>

Additional material and information about *Physiological Genomics* can be found at:

<http://www.the-aps.org/publications/pg>

This information is current as of April 14, 2006 .

Detection of differential gene expression in brown adipose tissue of hibernating arctic ground squirrels with mouse microarrays

Jun Yan,¹ Adlai Burman,¹ Calen Nichols,² Linda Alila,² Louise C. Showe,² Michael K. Showe,² Bert B. Boyer,¹ Brian M. Barnes,¹ and Thomas G. Marr¹

¹Institute of Arctic Biology, University of Alaska Fairbanks, Fairbanks, Alaska; and ²Wistar Institute, Philadelphia, Pennsylvania

Submitted 19 October 2005; accepted in final form 1 February 2006

Yan, Jun, Adlai Burman, Calen Nichols, Linda Alila, Louise C. Showe, Michael K. Showe, Bert B. Boyer, Brian M. Barnes, and Thomas G. Marr. Detection of differential gene expression in brown adipose tissue of hibernating arctic ground squirrels with mouse microarrays. *Physiol Genomics* 25: 346–353, 2006. First published February 7, 2006; doi:10.1152/physiolgenomics.00260.2005.—Hibernation is an energy-saving strategy adopted by a wide range of mammals to survive highly seasonal or unpredictable environments. Arctic ground squirrels living in Alaska provide an extreme example, with 6- to 9-mo-long hibernation seasons when body temperature alternates between levels near 0°C during torpor and 37°C during arousal episodes. Heat production during hibernation is provided, in part, by nonshivering thermogenesis that occurs in large deposits of brown adipose tissue (BAT). BAT is active at tissue temperatures from 0 to 37°C during rewarming and continuously at near 0°C during torpor in subfreezing conditions. Despite its crucial role in hibernation, the global gene expression patterns in BAT during hibernation compared with the nonhibernation season remain largely unknown. We report a large-scale study of differential gene expression in BAT between winter hibernating and summer active arctic ground squirrels using mouse microarrays. Selected differentially expressed genes identified on the arrays were validated by quantitative real-time PCR using ground squirrel specific primers. Our results show that the mRNA levels of the genes involved in nearly every step of the biochemical pathway leading to nonshivering thermogenesis are significantly increased in BAT during hibernation, whereas those of genes involved in protein biosynthesis are significantly decreased compared with summer active animals in August. Surprisingly, the differentially expressed genes also include adipocyte differentiation-related protein or adipophilin (*Adfp*), gap junction protein 1 (*Gjal*), and secreted protein acidic and cysteine-rich (*Sparc*), which may play a role in enhancing thermogenesis at low tissue temperatures in BAT.

metabolism; protein biosynthesis; thermogenesis

TO SURVIVE ANTICIPATED FAMINE in highly seasonal or unpredictable environments, a wide range of mammalian species have evolved the energy-saving strategy known as hibernation. Arctic ground squirrels (*Spermophilus parryii*) living near the edge of their northernmost distribution in Alaska provide an extreme example of hibernation. Over the long arctic winter, these ground squirrels spend as long as 9 mo hibernating in shallow burrows above the permafrost. As air temperature decreases to –40°C and soil temperature down to –18°C, arctic ground squirrels enter torpor by decreasing rates of heat production and metabolism and lowering core body temperature to as low

as –2.9°C (3). Torpor is interrupted every 10–21 days throughout hibernation by arousal episodes, however, as arctic ground squirrels spontaneously rewarm to euthermic body temperature (36–37°C) and maintain that temperature for 15–24 h before slowly reentering torpor.

Once called the “hibernation gland,” brown adipose tissue (BAT) was originally observed in hibernators. In hibernating animals and most mammalian neonates, BAT is essential for heat production through nonshivering thermogenesis (NST). BAT can be found in body regions including interscapular, periaortic, perirenal, and intercostal regions (11). BAT mainly consists of brown adipocytes, endothelial cells, interstitial cells, and preadipocytes that can divide and differentiate to form new brown adipocytes. In contrast to white adipose tissue (WAT), BAT is richly vascularized and densely packed with mitochondria, which give rise to its brown color. Brown adipocytes in the BAT contain many small lipid droplets (multilocular), whereas white adipocytes in WAT contain one big lipid droplet (unilocular). In BAT, uncoupling protein 1 (UCP1), a BAT-specific protein, transports protons or proton equivalents across the mitochondria inner membrane without synthesizing ATP, thus resulting in part of the energy stored in the proton gradient being dissipated as heat.

BAT deposits persist in adult hibernators year round, although their mass, density of mitochondria, and UCP1 content increase two- to threefold in fall before hibernation (5, 24). Active NST in BAT at euthermic tissue temperatures during summer occurs under the circumstances of cold stress or diet-induced thermogenesis. NST in hibernation, however, occurs in BAT at tissue temperatures that can vary from 0 to 37°C as animals rewarm over 3–6 h during arousals and also continuously over weeks at tissue temperatures near 0°C in steady-state conditions during torpor in animals hibernating in subfreezing environmental temperatures (9). It is not known whether different gene products are required for active thermogenesis in tissue temperatures of 0 vs. 37°C.

The interspersed phylogenetic distribution of hibernating and nonhibernating species has led to the hypothesis that hibernation phenotype results from the differential expression of existing genes rather than the creation of novel genes (6, 12, 27). In support of this hypothesis, a number of differentially expressed genes of known function have been identified in tissues of different hibernating species at both mRNA and protein levels (6, 12). A switch from carbohydrate metabolism to fatty acid metabolism during hibernation has been demonstrated in various tissues (2, 4, 26, 32). A limited number of genes including muscle- and heart-type fatty acid binding protein, adipose-type fatty acid binding protein, cytochrome-c oxidase subunit 1, ATP synthase 6/8, and peroxisome prolifer-

Article published online before print. See web site for date of publication (<http://physiolgenomics.physiology.org>).

Address for reprint requests and other correspondence: J. Yan, Inst. of Arctic Biology, 311 Irving Bldg., Univ. of Alaska Fairbanks, Fairbanks, AK 99775 (e-mail: fsj1@uaf.edu).

erator-activated receptor (PPAR)- γ have been reported to be differentially expressed in BAT during hibernation (14, 19, 20). These molecular studies on hibernation have focused on the analysis of one or a few candidate genes at a time. Broader, unbiased cDNA screening has been used in several studies at the mRNA level (2, 15, 17, 20). A proteomic approach using two-dimensional gels followed by tandem mass spectrometry has been carried out to identify differentially expressed liver proteins (16). Currently, several investigators are pursuing the global analysis of gene expression pattern in different hibernating species (8, 31).

Microarrays provide an efficient genomic approach for screening a large number of genes for differential expression. The major difficulty in applying microarray technology to hibernation studies is the lack of comprehensive genomic sequences for the hibernating animals of interest. An alternative approach is to use heterologous arrays consisting of probes from a related model organism. Previously, Hittel and Storey (19) successfully identified the upregulation of muscle- and heart-type and adipose-type fatty acid binding proteins in BAT of thirteen-lined ground squirrels (*Spermophilus tridecemlineatus*) with a commercial rat cDNA array. As demonstrated by the partial mRNA sequences of the 81 genes (GenBank accession nos. DQ333962–DQ334051) in arctic ground squirrel that we sequenced in our pilot study, mouse (*Mus musculus*) shares on average 89% mRNA sequence identities with arctic ground squirrel at the nucleotide level (see Supplemental Table S1, available at the *Physiological Genomics* web site).¹ Mouse microarrays covering a large number of the genes in the mouse genome have been developed and used in various studies. Our strategy was to screen for candidate genes that may be differentially expressed in hibernating arctic ground squirrels by large-scale mouse microarray experiments and then to validate the selected candidate genes by quantitative real-time PCR using ground squirrel-specific primer pairs.

MATERIALS AND METHODS

Animals. Arctic ground squirrels were trapped in summer in the Alaska Range (64°N 146°W, elevation 850 m) or on the North Slope of Alaska near Toolik Lake (68°N 149°W, elevation 809 m) and transported to University of Alaska Fairbanks. Animals sampled during hibernation were housed at $5 \pm 2^\circ\text{C}$ with a 4:20-h light-dark photoperiod and were given Mazuri Rodent Chow and water ad libitum and provided with sunflower seeds, carrots, and apple slices. Animals sampled to represent the summer active season were captured in August, housed at 18°C with constant light, provided with food as above, and killed within 5 days. Animals sampled to represent hibernation were inspected twice daily, and wood shavings were placed on the dorsal surface of hibernating animals to assess the pattern of torpor bouts and the occurrence of arousal episodes. Tissues were collected from hibernators after no fewer than 5 days of continuous torpor in at least the third torpor bout of the winter hibernation season. Torpid animals ($n = 5$) were euthanized by decapitation without anesthesia after verification of core body temperatures $<7^\circ\text{C}$ with a rectal thermometer. Summer active animals ($n = 3$) were anesthetized with halothane and decapitated. BAT was rapidly dissected, frozen in liquid nitrogen, and stored at -70°C until total RNA was isolated at a later date. To illustrate the pattern and extent of body

temperature change during a natural hibernation season of arctic ground squirrels, a small (10 g) temperature-sensitive data logger was implanted in the peritoneal cavity of a free-living adult male that was released at its home burrow and then recaptured a year later to retrieve the logger. Further details about the environment of the ground squirrel and the logger and surgery procedure were described previously (23). Animal protocols were approved by the University of Alaska Fairbanks Institutional Animal Care and Use Committee.

Sample preparation. Total RNA was prepared from frozen tissue by homogenizing directly in Tri-reagent (Molecular Research Center), using a Polytron (Brinkman) with a 7-mm generator (Kinematica). RNA was processed according to the manufacturer's directions, and RNA quality was assessed by 1% agarose gel electrophoresis using SYBR Green II poststaining (Cambrex). All RNA samples were subsequently linearly amplified with a modified T7 Eberwine procedure (30), and 2 μg of the amplified RNA was labeled with 60 μCi of [^{33}P]dCTP as previously described (21).

Microarrays. Nylon microarrays (MA07, MA08, MA10, and MA11) printed with PCR-amplified mouse cDNAs were obtained from the Wistar Genomics Facility (<http://www.wistar.upenn.edu/genomics/>). These arrays carry $\sim 38,000$ clones (9,600 on each array) including 4,392 sequence-verified clones (Research Genetics/Invitrogen mouse plates 1–17 and 51–79); 11,000 clones from the Mouse Brain Molecular Anatomy Project ("BMAP" clones, Research Genetics/Invitrogen); 15,000 sequence-verified clones from the National Institute of Aging (NIA Mouse 15K) mouse cDNA development libraries created from pre- and periimplantation embryos, embryonic day 12.5 female gonad/mesonephros, and newborn ovary; and 7,000 sequence-verified clones from the NIA 7.4K Mouse cDNA clone set with no redundancy within the set or with NIA Mouse 15K (<http://lgsun.grc.nia.nih.gov/cDNA/cDNA.html>). The NIA clones are reported to be primarily full length. An additional 700 selected clones with functions related to the immune system were purchased from Research Genetics/Invitrogen. The gene lists, including GenBank accession numbers and Unigene build 134 cluster assignments, are available at http://showelab.wistar.upenn.edu/Wistar_Showe_Lab_Gene_Lists.htm.

Hybridization and washing. Filters MA07, MA08, and MA11 were hybridized with the same labeled target in the same hybridization bottle with filters separated by nylon mesh. Filter MA10 was hybridized separately at an earlier date with the same aRNA preparation as used for the rest of the filters. The hybridization was carried out for 16 h at 42°C followed by 24 h at 35°C in 5 ml of MicroHyb buffer (Research Genetics). The lower temperatures and extended hybridization times were implemented to promote cross-species hybridization. Filters from both hybridizations were batch washed in a large container for consistency. Filters were rinsed at room temperature with $2\times$ SSC-1% SDS to remove residual probe and MicroHyb solution and then transferred to preheated wash solutions in a temperature-controlled shaking water bath. One liter of solution was used for filters in the batch. Filters were washed twice for 30 min in $2\times$ SSC-1% SDS at 50°C and then once for 30 min in $0.5\times$ SSC-0.5% SDS at 55°C . Filters were then exposed to phosphorimager screens for 6 days and scanned at 50- μm resolution in a Storm Phosphorimager. After the first scanning, the filters were rewashed in $0.1\times$ SSC-0.5% SDS for 30 min at 55°C and then reexposed to the Phosphorimager screens for 11 days and scanned for the second time. Images of the first scanning were used for the MA10 filter. Images of the second scanning were used for MA07, MA08, and MA11 filters for higher stringency. Image analysis was performed with the ImaGene program (Biodiscovery).

Microarray data analysis. Only spots on the array satisfying flag = 0 (nonempty spot) and signal median > background median were included in the analysis. Local background median was subtracted from signal median as background-corrected signal. Background-corrected signals were divided by their median on the array as the normalized expression values. The normalized expression values of

¹ The Supplemental Material for this article (Supplemental Tables S1 and S2) is available online at <http://physiolgenomics.physiology.org/cgi/content/full/00260.2005/DC1>.

technical replicas (samples split from the same total RNA extraction) were averaged as the final expression values and then again normalized. The final normalized expression values were \log_2 transformed. Log fold change is defined as the difference between the means of \log_2 -transformed expression values in the winter hibernating group and the summer active group, i.e., $[\log_2(\text{expression value})]_{\text{hibernating}} - [\log_2(\text{expression value})]_{\text{active}}$. The P value of the two-tailed Student's t -test was calculated by Excel (Microsoft). We used $P < 0.05$ and $|\log \text{fold change}| > 1$ as the criteria for significant difference. GenBank accession numbers of all probes on the arrays were uploaded to Stanford Source (<http://source.stanford.edu>) to obtain the gene names and symbols. We combined multiple probes for the same gene and removed the unannotated (no gene symbols assigned) probes. When evaluating multiple probes corresponding to the same gene, we chose the probe with the lowest P value. The significant genes were uploaded to GMiner (<http://discover.nci.nih.gov/gominer/index.js>) to identify the significant Gene Ontology (GO) categories. The enrichment in each category was calculated as the proportion of changed genes in the category relative to the expected proportion on the arrays: the ratio of changed genes in the category divided by the total number of genes in the category, divided by the same ratio for the genes on the entire arrays. The P value of the significance of each GO category was calculated by one-sided Fishers exact test (33). All microarray data series were submitted to NCBI Gene Expression Omnibus (GEO) with accession number GSE3426.

Primer design. The specificity of real-time PCR requires using exact or near-exact gene-specific primer sequences. *Spermophilus lateralis* and *Spermophilus tridecemlineatus* share on average 99% sequence identities with the arctic ground squirrel (Supplemental Table S1). We combined 81 arctic ground squirrel sequences (GenBank accession nos. DQ333962–DQ334051) sequenced from our pilot study with 8,816 *S. lateralis* sequences and 2,343 *S. tridecemlineatus* sequences downloaded from GenBank into a ground squirrel database. The mouse RefSeq sequences of the significant genes identified on the arrays were searched against the ground squirrel database with the BLAST program (1). Among the genes with significant ground squirrel sequence homology, 33 genes were selected for real-time PCR assay based on a broad representation for important functional categories as discussed in RESULTS. This includes five in fatty acid metabolism, four in the tricarboxylic acid (TCA) cycle, one in anaerobic metabolism, four in electron transport, one in ATP biosynthesis, two in transport, one heat shock protein, one antioxidant protein, three in protein biosynthesis, five in BAT differentiation and remodeling, and six others. Three additional genes (*Ucp1*, *Hsl*, and *Fabp4*) that were not present on the arrays were also tested in real-time PCR. The identified ground squirrel sequence was also aligned to possible paralogous genes (gene homologs within the same species, isozymes, for example). The sequence regions that are highly conserved among paralogous genes were avoided in primer design. Gene-specific primers were designed with Primer Express software (Applied Biosystems). For *Acadm*, *Sucla2*, *Suclg1*, *Actb*, and *Ucp1*, primers were designed from arctic ground squirrel sequences. For all the rest of the genes except *Mdh1*, primers were designed from *S. lateralis* or *S. tridecemlineatus* sequences. For *Mdh1*, primers designed from *S. lateralis* sequence (GenBank accession no. CO737160) failed in real-time PCR reaction. We suspect that this sequence either is an artifact or has large sequencing errors. In contrast, the primers designed from the conserved regions of *Mdh1* in human, mouse, and rat were successful in real-time PCR reaction. The sequences of primer pairs and GenBank accession numbers of the orthologous sequences and the sources from which they are derived are listed in Supplemental Table S2.

Real-time PCR. We carried out real-time PCR on the same samples used in the array experiments. Two-step real-time PCR was performed on an ABI-7900 HT system (Applied Biosystems) with SYBR Green reagent (Applied Biosystems). The density of total RNA of each sample was measured by spectrometer. The cDNA was synthesized

from 0.5 μg of total RNA of each sample, using Multiscribe reverse transcriptase (Applied Biosystem) with oligo d(T)₁₆ primer in a 20- μl reaction at 25°C for 10 min, 48°C for 30 min, and 95°C for 5 min. The synthesized cDNA was diluted 10 \times with RNase-free water into a 200- μl solution. Five microliters (5 μl) of diluted cDNA solution were used in each twenty-five-microliter (25- μl) real-time PCR reaction. Cycle parameters were 95°C for 10-min hot start and 40 cycles of 95°C for 15 s and 60°C for 1 min. The controls with no cDNA templates were performed to rule out contamination. The controls with no reverse transcriptase but all other components were used to rule out false amplification from genomic DNA. PCR product specificity was checked by melting curve analysis and gel electrophoresis.

Comparisons between arrays and real-time PCR. The critical threshold (C_T) value is the PCR cycle number at which PCR growth curve crosses a defined threshold in the linear range of reaction. It can be related to gene expression values by the formula $\log_2(\text{expression value}) = C - C_T$, where C is the normalization constant. Because we normalized the samples by starting with the same amount of total RNA, C is constant across the samples for a specific gene and irrelevant for the following statistical analysis. A two-tailed Student's t -test on $-C_T$ was used directly.

RESULTS

The body temperature of a typical free-living male arctic ground squirrel during hibernation is shown in Fig. 1. This 1-kg ground squirrel maintained core body temperature between 35 and 40°C during August and September before becoming sequestered in its burrow and beginning hibernation on October 1, 1998. For the duration of the 6-mo hibernation season, body temperature varied from 3°C to -2°C during torpor bouts that lasted 10–24 days between nine arousal episodes when body temperature returned to euthermic temperatures for 10–15 h.

Four Wistar mouse arrays (MA07, MA08, MA10, MA11) each carrying 9,600 probes were used to screen the differentially expressed genes between winter hibernating and summer active arctic ground squirrels. We used $P < 0.05$ and $|\log \text{fold change}| > 1$ as the criteria for significant difference. Combining all four arrays, we identified 668 probes that were significantly overexpressed during hibernation and 390 probes that

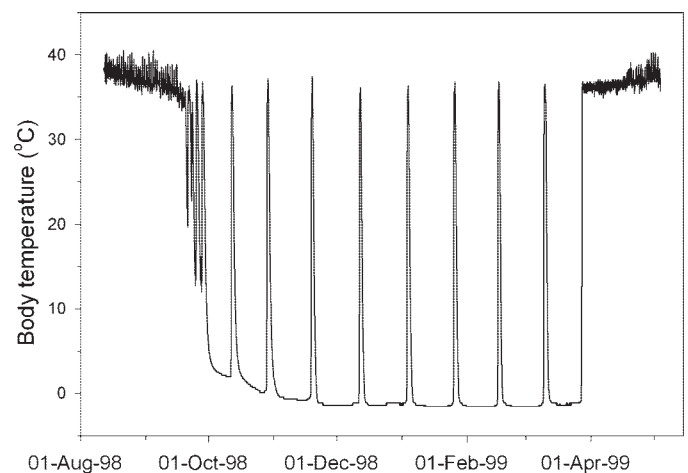


Fig. 1. Core body temperature change in a free-living male arctic ground squirrel overwintering near the shore of Toolik Lake in northern Alaska. The hibernation season is composed of several bouts of daily torpor followed by extended bouts of multiday torpor interrupted by 8 arousal episodes, when body temperature briefly returns to euthermic levels.

were significantly underexpressed during hibernation among the 38,400 probes on the arrays.

When there were multiple probes corresponding to the same gene on the arrays, their results were often consistent. For example, five of eight probes distributed across four arrays corresponding to Succinate-CoA ligase, ADP-forming, β -subunit (*Sucla2*) showed significant overexpression in winter hibernating squirrels. This indicates that our array results are highly reproducible. After we removed the unannotated probes and combined multiple probes corresponding to the same gene on the arrays, we identified 408 genes overexpressed during hibernation and 217 genes underexpressed during hibernation among the 11,670 annotated genes on the arrays. The top five overexpressed genes during hibernation according to their log fold changes are *Sucla2* (4.37), Gap junction protein $\alpha 1$ (*Gjal*, 3.70), Growth hormone-inducible transmembrane protein (*Ghitm*, 3.47), Progesterone receptor membrane component 1 (*Pgrmc1*, 3.39), and Dihydropyrimidinase (*Dld*, 3.27), where the numbers in parentheses are log fold changes. The top five underexpressed genes during hibernation are Eukaryotic translation elongation factor 1 γ (*Eef1g*, -2.95), expressed sequence AV312086 (-2.52), Ribosomal protein S10 (*Rps10*, -2.36), Ribosomal protein L35 (*Rpl35*, -2.36), and Syntaxin 6 (*Stx6*, -2.34).

The significant differentially expressed genes identified on the arrays were classified according to their GO categories. The significantly overrepresented GO categories and their gene members are listed in Tables 1 and 2. The important functional categories are summarized below.

Metabolism. The genes involved in fatty acid metabolism, the tricarboxylic acid (TCA) cycle, electron transport, and ATP synthesis were significantly overexpressed in hibernating animals compared with summer active animals. These include acyl-CoA synthetase long-chain (*Acs1l*), acyl-CoA dehydrogenase (*Acadm*, *Acadl*), and acyl-CoA acyltransferase (*Acaa2*) in fatty acid metabolism; succinate-CoA ligase (*Sucla2*, *Suclg1*), isocitrate dehydrogenase (*Idh3a*, *Idh3b*), and malate dehydrogenase (*Mdh1*) in TCA cycle; cytochrome *c* somatic (*Cyca*), cytochrome *b₅* (*Cyb5*), NADH dehydrogenase (*Ndufa8*, *Ndufb9*), ubiquinol-cytochrome *c* reductase (*Uqcrrb*, *Uqcrc2*, *Uqcrfs1*, *Uqcrh*), and cytochrome-*c* oxidase (*Cox6c*, *Cox7c*, *Cox17*) in electron transport; and ATP synthase (*Atp5a1*, *Atp5b*, *Atp5f1*) in ATP synthesis. Lactate dehydrogenase (*Ldha*, *Ldhb*) involved in anaerobic metabolism was significantly overexpressed during hibernation. Methylmalonyl-CoA mutase (*Mut*) was also significantly overexpressed during hibernation.

Table 1. Significant GO categories classified by GOMiner

GO Category	Total Genes on Arrays	Differentially Expressed Genes	Enrichment	Log ₁₀ (P)
TCA cycle	22	6	6.87	-3.79
Electron transport	177	17	2.42	-3.22
ATP synthesis	21	5	5.95	-2.93
Fatty acid metabolism	88	10	2.86	-2.62
Protein biosynthesis	357	27	3.45	-8.04

The enrichment in each category was calculated as the proportion of changed genes in the category relative to the expected proportion on the arrays. The *P* value of the significance of each Gene Ontology (GO) category was calculated by 1-sided Fishers exact test (33). TCA, tricarboxylic acid.

Protein biosynthesis. The genes involved in protein biosynthesis were significantly underexpressed during hibernation, including Eukaryotic translation elongation factor (*Eef1d*, *Eef1g*), translation initiation factor (*Eif3s5*), and a total of 23 ribosomal proteins.

Transport. Heart- and muscle-type fatty acid binding protein (*Fabp3*) responsible for intracellular transport of fatty acids was significantly overexpressed during hibernation. Solute carrier family 25 member 20 or carnitine/acyl-carnitine translocase (*Slc25a20* or *Cact*) located at the mitochondrial inner membrane, where it transfers fatty acylcarnitines into mitochondria, was also significantly overexpressed during hibernation.

Heat shock proteins. There were 37 heat shock proteins present on the arrays. Heat shock 70-kDa protein 9A (*Hspa9a*) and DnaJ (Hsp40) homolog, subfamily B, member 9 (*Dnajb9*) were overexpressed during hibernation, whereas heat shock 10-kDa protein 1 (*Hspe1*) and heat shock 90-kDa protein 1 α (*Hspca*) were underexpressed during hibernation.

Antioxidant proteins. Two isozymes of superoxide dismutase, *Sod1* and *Sod2*, were both overexpressed during hibernation.

BAT differentiation and remodeling. Adipocyte differentiation-related protein or adipophilin (*Adfp*) and Gap junction protein 1 (*Gjal*) were overexpressed during hibernation. Secreted protein acidic and cysteine-rich (*Sparc*) and β -actin (*Actb*) were significantly underexpressed during hibernation.

Others. Asparagine synthetase (*Asns*) and Tyrosine 3-monooxygenase/tryptophan 5-monooxygenase activation proteins (*Ywhae*, *Ywhag*, *Ywhaz*) were overexpressed during hibernation, whereas transforming growth factor $\beta 1$ -induced transcript 4 (*Tgfb1i4*) and hemoglobin $\alpha 1$ (*Hba1*) were underexpressed during hibernation.

Quantitative real-time PCR was used to test 33 genes differentially expressed during hibernation, including 28 overexpressed and 5 underexpressed genes that were identified on the arrays. Ground squirrel specific primer pairs were used to guarantee the specificity of PCR reactions. The results are listed in Table 3. In the quantitative real-time PCR assay, all 33 genes showed changes of expression levels between hibernating animals and summer active animals in the same direction as the array results. Twenty-six genes (79%) showed significant differences ($P < 0.05$) in real-time PCR assay. Among the other seven genes, *Atp5b* ($P = 0.08$), *Cox6c* ($P = 0.06$), and *Tgfb1i4* ($P = 0.06$) showed less significant differences ($P < 0.1$), whereas the differences in *Acaa2*, *Suclg1*, *Idh3a*, and *Dld* were not significant ($P > 0.1$) in the real-time PCR assay. The log fold changes of 33 genes in the real-time PCR are plotted against those on the arrays in Fig. 2. The linear fit of the plot gives $y = 0.5885x + 0.0943$ ($R^2 = 0.4678$), where *y* is the real-time PCR result and *x* is the array result. Three additional genes that were absent on the arrays (*Ucp1*, *Hsl*, *Fabp4*) were also tested in the real-time PCR assay. The *Ucp1* level was increased by 5.67-fold ($P < 0.001$), and the *Hsl* level was increased by 2.96-fold ($P = 0.03$), whereas the *Fabp4* level was not significantly changed ($P = 0.805$) in hibernating animals compared with summer active animals.

DISCUSSION

Our results are consistent with the previous studies of differential gene expression in BAT during hibernation. The

Table 2. Genes in each significant GO category identified by GOMiner

GO Category	Gene Name	Gene Symbol	Accession No.	Log Fold Change	P Value
TCA cycle	Dihydrolipoamide S-succinyltransferase	<i>Dlst</i>	AI849904	2.30	0.002
	Isocitrate dehydrogenase 3 (NAD+)α	<i>Idh3a</i>	BG077913	1.69	0.002
	Isocitrate dehydrogenase 3 (NAD+) β	<i>Idh3b</i>	AU019946	1.37	0.04
	Malate dehydrogenase 1	<i>Mdh1</i>	BG064914	1.50	0.004
	Succinate-CoA ligase, ADP-forming, β-subunit	<i>Sucla2</i>	AI835580	4.37	<0.001
	Succinate-CoA ligase, GDP-forming, α-subunit	<i>Suclg1</i>	BG071511	1.11	0.03
Electron transport	Cytochrome-c oxidase, subunit VIc	<i>Cox6c</i>	BG085306	2.21	<0.001
	Cytochrome-c oxidase, subunit VIIc	<i>Cox7c</i>	BG077312	1.64	0.004
	Cytochrome b ₅	<i>Cyb5</i>	BG065259	1.30	<0.001
	Cytochrome c, somatic	<i>Cycc</i>	BG063100	3.25	<0.001
	Dihydrolipoamide dehydrogenase	<i>Dld</i>	AI847502	3.27	0.001
	Electron transferring flavoprotein, dehydrogenase	<i>Etfldh</i>	BG083466	1.62	0.02
	Glycerol phosphate dehydrogenase 2, mitochondrial	<i>Gpd2</i>	AI846919	1.62	0.006
	NADH dehydrogenase (ubiquinone) 1β subcomplex, 9	<i>Ndufb9</i>	BG087636	1.98	0.004
	NADH dehydrogenase (ubiquinone) Fe-S protein 1	<i>Ndufs1</i>	BG088100	1.28	0.03
	NADH dehydrogenase (ubiquinone) 1α subcomplex, 8	<i>Ndufa8</i>	BG087056	1.73	0.005
	Thioredoxin 1	<i>Txn1</i>	AI844775	1.27	0.001
	Ubiquinol-cytochrome c reductase binding protein	<i>Uqcrb</i>	BG085012	2.80	0.009
	Ubiquinol cytochrome c reductase core protein 2	<i>Uqcrc2</i>	BG075001	1.14	0.006
	Ubiquinol-cytochrome c reductase, Rieske iron-sulfur polypeptide 1	<i>Uqcrcf1</i>	AI850420	1.26	0.04
	Ubiquinol-cytochrome c reductase hinge protein	<i>Uqcrh</i>	AI843761	1.06	0.01
ATP biosynthesis	ATP synthase, H ⁺ transporting, mitochondrial F1 complex, α-subunit, isoform 1	<i>Atp5a1</i>	AW412466	2.77	0.007
	ATP synthase, H ⁺ transporting mitochondrial F1 complex, β-subunit	<i>Atp5b</i>	BQ559302	2.29	<0.001
	ATP synthase, H ⁺ transporting, mitochondrial F0 complex, subunit b, isoform 1	<i>Atp5fl</i>	AI837594	1.39	0.04
	ATPase, H ⁺ transporting, V0 subunit D isoform 1	<i>Atp6v0dl</i>	AU043006	2.02	0.003
	ATPase, H ⁺ transporting, V1 subunit E isoform 1	<i>Atp6v1el</i>	AI844873	1.89	0.04
Fatty acid metabolism	Acetyl-CoA acyltransferase 2	<i>Acaa2</i>	BG085346	1.23	0.007
	Acetyl-CoA dehydrogenase, long chain	<i>Acadl</i>	C79809	2.32	0.004
	Acetyl-CoA dehydrogenase, medium chain	<i>Acadm</i>	AI840666	2.29	<0.001
	Acyl-CoA thioesterase 2	<i>Acate2</i>	BG063815	1.04	0.003
	Acyl-CoA synthetase long-chain family member 1	<i>Acs1l</i>	BG074754	1.96	<0.001
	Caveolin, caveolae protein 1	<i>Cav1</i>	BG083456	1.49	0.05
	Glycerol-3-phosphate acyltransferase, mitochondrial	<i>Gpam</i>	BQ552668	1.38	0.04
	Protein kinase, cAMP-dependent regulatory, type IIβ	<i>Prkar2b</i>	AI851427	1.25	0.02
	Sterol carrier protein 2, liver	<i>Scp2</i>	BG086835	1.70	0.007
	Protein biosynthesis	Acidic ribosomal phosphoprotein P0	<i>Arbp</i>	BG064817	-1.16
UDP-Gal:betaGlcNAc β 1,3-galactosyltransferase, polypeptide 3		<i>B3galt3</i>	AI841494	-1.71	0.008
Eukaryotic translation elongation factor 1δ		<i>Eef1d</i>	AI839632	-2.17	0.02
Eukaryotic translation elongation factor 1γ		<i>Eef1g</i>	BG072780	-2.95	<0.001
Eukaryotic translation initiation factor 3, subunit 5		<i>Eif3s5</i>	AI836722	-1.25	0.03
Finkel-Biskis-Reilly murine sarcoma virus, ubiquitously expressed; ribosomal protein S30		<i>Fau</i>	BG087448	-1.76	0.004
Laminin receptor 1 (ribosomal protein SA)		<i>Lamr1</i>	BG072822	-1.70	<0.001
Ribosomal protein L10		<i>Rpl10</i>	BG085975	-1.84	0.005
Ribosomal protein L10A		<i>Rpl10a</i>	AI849117	-1.00	0.04
Ribosomal protein L12		<i>Rpl12</i>	AI851649	-1.15	0.04
Ribosomal protein L13A		<i>Rpl13a</i>	BG087204	-1.07	0.02
Ribosomal protein L18A		<i>Rpl18a</i>	BG072556	-1.85	0.002
Ribosomal protein L3		<i>Rpl3</i>	BG072595	-1.65	<0.001
Ribosomal protein L31		<i>Rpl31</i>	BG086430	-1.47	0.002
Ribosomal protein L32		<i>Rpl32</i>	AW556391	-1.66	<0.001
Ribosomal protein L35		<i>Rpl35</i>	BG072983	-2.36	0.002
Ribosomal protein L36		<i>Rpl36</i>	BG072993	-2.10	0.01
Ribosomal protein L4		<i>Rpl4</i>	BG086419	-1.29	0.03
Ribosomal protein L17		<i>Rpl7</i>	BG072985	-1.11	0.04
Ribosomal protein, large, P1		<i>Rplp1</i>	BG074911	-1.99	<0.001
Ribosomal protein, large, P2		<i>Rplp2</i>	AI853822	-1.93	0.01
Ribosomal protein S14		<i>Rps14</i>	BG086818	-1.67	<0.001
Ribosomal protein S15		<i>Rps15</i>	BG087421	-2.24	0.002
Ribosomal protein S16		<i>Rps16</i>	BG072615	-1.58	0.005
Ribosomal protein S5		<i>Rps5</i>	BI076433	-1.45	0.01
Ribosomal protein S8		<i>Rps8</i>	BG085869	-1.38	0.002
Ribosomal protein S9		<i>Rps9</i>	BG067495	-1.58	0.009

Genes in each significant GO category identified by GOMiner and their log fold changes and P values in expression level differences on the arrays between hibernating animals and summer active animals are shown. Note that *Acadl*, *Acadm*, and *Cyb5* are involved in both electron transport and fatty acid metabolism.

Table 3. Real-time PCR validation of 33 selected genes

Genes		Array Experiment		Real-Time PCR	
Name	Symbol	Log fold change	P value	Log fold change	P value
Acetyl-CoA synthetase long-chain family member 1	<i>Acs11</i>	1.96	<0.001	1.69	<0.001
Acetyl-CoA dehydrogenase, median chain	<i>Acadm</i>	2.29	<0.001	1.28	<0.001
Sterol carrier protein 2	<i>Scp2</i>	1.70	0.007	0.717	0.039
Acyl-CoA thioesterase 2	<i>Acate2</i>	1.04	0.003	1.88	0.008
Acetyl-CoA acyltransferase 2	<i>Acaa2</i>	1.23	0.007	0.38	0.20
Succinate-CoA ligase, ADP-forming	<i>Suc1a2</i>	4.37	<0.001	2.47	<0.001
Succinate-CoA ligase, GDP-forming, α -subunit	<i>Suc1g1</i>	1.11	0.03	0.10	0.65
Isocitrate dehydrogenase 3 (NAD+) α	<i>Idh3a</i>	1.69	0.002	0.34	0.45
Malate dehydrogenase 1	<i>Mdh1</i>	1.50	0.004	1.05	0.037
Cytochrome-c oxidase, subunit VIc	<i>Cox6c</i>	2.21	<0.001	0.53	0.055
Dihydroipoamide dehydrogenase	<i>Dld</i>	3.27	0.001	0.44	0.18
Cytochrome c, somatic	<i>Cycc</i>	3.25	<0.001	0.72	0.023
NADH dehydrogenase 1 α 8	<i>Ndufa8</i>	1.73	0.005	2.14	0.002
Lactate dehydrogenase α	<i>Ldha</i>	1.11	0.01	0.979	0.005
ATP synthase, H ⁺ transporting mitochondrial F1 complex, β -subunit	<i>Atp5b</i>	2.29	<0.001	1.51	0.08
Fatty acid binding protein 3	<i>Fabp3</i>	2.54	0.004	4.26	<0.001
Carnitine/acylcarnitine translocase	<i>Cact</i>	1.74	<0.001	2.05	0.009
Heat shock protein 9A	<i>Hspa9a</i>	2.62	<0.001	0.76	0.006
Superoxide dismutase 2	<i>Sod2</i>	1.59	0.005	1.21	0.001
Translation elongation factor 1 α 1	<i>Eef1a1</i>	-0.945	0.02	-0.951	0.03
Ribosomal protein S16	<i>Rps16</i>	-1.58	0.005	-0.881	0.005
Ribosomal protein L3	<i>Rpl3</i>	-1.65	<0.001	-0.67	0.023
Adipose differentiation-related protein	<i>Adfp</i>	0.833	0.01	3.26	<0.001
Growth hormone-inducible transmembrane protein	<i>Ghitm</i>	2.85	0.003	1.40	0.01
Gap junction protein α 1	<i>Gjal</i>	2.74	0.001	2.17	0.002
Secreted protein, acidic, cysteine rich	<i>Sparc</i>	-1.52	0.003	-2.14	<0.001
β -Actin	<i>Actb</i>	-1.21	0.004	-1.16	0.04
Asparagine synthetase	<i>Asns</i>	1.32	0.003	1.65	0.005
Tyrosine 3-monooxygenase/tryptophan 5-monooxygenase activation protein, ϵ polypeptide	<i>Ywhae</i>	1.26	0.007	0.57	0.039
Methylmalonyl-CoA mutase	<i>Mut</i>	2.21	<0.001	0.81	0.026
Protein tyrosine phosphatase 4a1	<i>Ptp4a1</i>	1.29	<0.001	1.10	0.024
Transforming growth factor β 1 induced transcript 4	<i>Tgfb1i4</i>	-1.25	0.048	-0.80	0.06
RAB1, member RAS oncogene family	<i>Rab1</i>	1.94	<0.001	1.04	0.01

Comparison between array experiment and real-time PCR assay for 33 selected genes is shown. Log fold change in real-time PCR was calculated from the difference in $-C_T$ between hibernating animals and summer active animals, where C_T is critical threshold in real-time PCR. P value was calculated from 2-tailed Student's t -test.

overexpression of *Fabp3* during hibernation on our arrays is consistent with References 13 and 19. The overexpression of cytochrome-c oxidase and ATP synthase on our arrays is consistent with Reference 20. However, as pointed out in References 20 and 28, the protein level of ATP synthase is low in BAT because the major role of BAT is heat production through futile proton cycling. This disagreement may be due to regulation at the posttranscriptional level. The overexpression of two isozymes of superoxide dismutase (*Sod1* and *Sod2*)

during hibernation is consistent with Reference 10. Buzadzic et al. (10) showed that the activities of both *Sod1* and *Sod2* were increased in brown adipose tissue of European ground squirrels (*Spermophilus citellus*) during hibernation. Superoxide dismutase acts as an antioxidant to destroy the harmful superoxide radicals in the body. The increased level of the antioxidant can protect the tissue from reactive oxygen species generated as a result of the intense metabolic activity sustained by this tissue during arousal.

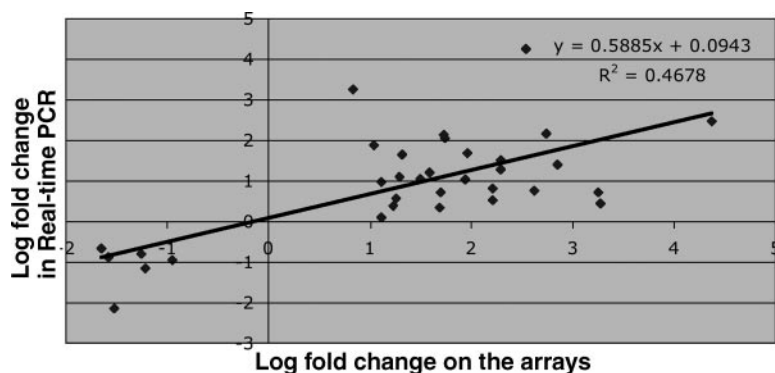


Fig. 2. Log fold changes of 33 genes on the arrays vs. those in real-time PCR assay. The P values of their gene expression changes on the arrays and in real-time PCR assay are shown in Table 3.

In BAT, NST is controlled by norepinephrine released by sympathetic nerves. Norepinephrine signaling through β_3 -adrenoceptor activates hormone-sensitive lipase (*Hsl*) to cleave the triglyceride stored in the lipid droplet in brown adipocytes into free fatty acid and glycerol. In our real-time PCR assay, the *Hsl* level was significantly increased in hibernating animals compared with summer active animals. In cytosol, free fatty acid is bound with fatty acid binding proteins. Two types of fatty acid binding proteins exist in BAT: muscle and heart type (*Fabp3*) and adipose type (*Fabp4*). Hittel and Storey (19) showed that both types of fatty acid binding proteins are overexpressed during hibernation. We also showed that *Fabp3* is overexpressed during hibernation on our arrays. Although *Fabp4* was not present on our arrays, *Fabp4* is not significantly overexpressed during hibernation in our real-time PCR assay. The fatty acid is activated to fatty acyl-CoA by acyl-CoA synthetases before entering mitochondria. On our arrays, acyl-CoA synthetase long-chain (*Acs11*) is overexpressed during hibernation. Fatty acyl-CoA is transformed to fatty acyl-carnitine by carnitine palmitoyltransferase I and then transported into the mitochondria through carnitine/acyl-carnitine translocase (*Cact*) and reconverted to fatty acyl-CoA by carnitine palmitoyltransferase II. This carnitine-mediated entry process is the rate-limiting step for fatty acid β -oxidation. On our arrays, *Cact* is significantly overexpressed during hibernation. After entering mitochondria, fatty acyl-CoA undergoes β -oxidation to generate acetyl-CoA. The enzymes involved in the first and last steps of the β -oxidation cycles, acyl-CoA dehydrogenase (*Acaadm*, *Acadl*) and acyl-CoA acyltransferase (*Acaa2*), are overexpressed during hibernation on our arrays. In mitochondria, acetyl-CoA is further oxidized in the TCA cycle. Three of the eight enzymes in the TCA cycle, succinate-CoA ligase (*Sucla2*, *Suclg1*), isocitrate dehydrogenase (*Idh3a*, *Idh3b*), and malate dehydrogenase (*Mdh1*), are significantly overexpressed during hibernation on our arrays. Both fatty acid β -oxidation and the TCA cycle lead to the formation of the reduced electron carrier FADH and NADH, which are then oxidized by the electron transport chain. All three enzymes in the electron transport chain, NADH dehydrogenase (*Ndufa8*, *Ndufb9*), ubiquinol-cytochrome *c* reductase (*Uqcrb*, *Uqcrc2*, *Uqcrfs1*, *Uqcrh*), and cytochrome-*c* oxidase (*Cox6c*, *Cox7c*, *Cox17*), are overexpressed during hibernation on our arrays. The respiration through the electron transport chain pumps protons out of the mitochondria matrix, leading to the formation of the proton gradient across the mitochondria membrane. As the protons or proton equivalents flow through *Ucp1*, the energy stored in the proton gradient is dissipated as heat. Although *Ucp1* was not present on our arrays, we used real-time PCR to show that it was indeed overexpressed during hibernation. It is remarkable that nearly every step in the biochemical pathway leading to NST is elevated in BAT during hibernation. Under the above-freezing conditions of this experiment, thermogenic activity in the BAT of animals sampled during torpor should have been low and only activated during arousal. There is evidence that the translation of mRNA into proteins is inhibited during torpor (18, 29). The underexpression of a large number of genes involved in protein biosynthesis on our arrays also supports this view. The elevated mRNA levels of the genes involved in NST may be important for rapid translation after arousal to high body temperature (22).

During hibernation NST has to work at tissue temperatures from 0 to 37°C in BAT, whereas the tissue temperature in BAT is always near 37°C in summer active animals. Among the differentially expressed genes identified on our arrays, some may potentially enhance the thermogenesis at low tissue temperature during hibernation. The overexpression of *adfp* gene during hibernation on our arrays indicates the enhanced brown adipocyte differentiation in BAT during hibernation. More mature adipocytes means higher thermogenic capacity in BAT. Gap junctions are intercellular channels for the diffusion of low-molecular-weight molecules between cells. *Gjal* or connexin 43, a member of the gap junction proteins, has been shown to be overexpressed in the heart of hibernating hamsters, which may help hamsters avoid fibrillation during hibernation and arousal (25). The overexpressed *Gjal* may enhance substrate transport through gap junctions in BAT and thus increase its thermogenic capacity during hibernation. *Sparc* is a matrix-associated protein that elicits changes in cell shape, inhibits cell cycle progression, and influences the synthesis of extracellular matrix. *Sparc* is underexpressed during hibernation on our arrays. Bradshaw et al. (7) showed that mice lacking *Sparc* exhibit an increase in the size and number of adipocytes. The underexpression of *Sparc* during hibernation may also play a role in the accumulation and differentiation of adipocytes in BAT. *Actb*, which is normally considered a housekeeping gene, is underexpressed during hibernation. This further suggests that BAT may have undergone structure remodeling to enable the differentiation and maturation of brown adipocyte to increase its thermogenic capacity at low tissue temperature during hibernation.

In conclusion, our microarray results not only agree with previous studies on BAT during hibernation but also have revealed the differential expression of a large number of genes not previously shown to be involved in hibernation. It is clear from this study that significant global changes occur at the mRNA level in BAT during hibernation. The fact that the genes involved in nearly every step of the biochemical pathway leading to NST are overexpressed in BAT during hibernation reflects the unique role of BAT as a "furnace" during hibernation. The differential expression of the genes involved in adipose differentiation, substrate transport, and structure remodeling may enhance the thermogenesis in BAT at low tissue temperature. Future studies including multiple stages throughout hibernation and concurring protein expression would give us a more complete understanding of the molecular mechanism underlying the hibernation phenotype.

ACKNOWLEDGMENTS

We thank Vadim Fedorov for help in RNA extraction.

GRANTS

We acknowledge support from National Institutes of Health Division of Research Resources Grant RR-16466-01 (T. G. Marr), National Science Foundation (NSF) Grant EPS-0092040 (T. G. Marr), Microarray Network Grant NSF-RCN 0090286 (M. K. Showe and B. B. Boyer), Department of Defense Experimental Program to Stimulate Competitive Research Grant N00014-01-1-0907 (B. B. Boyer), the University of Alaska Foundation (T. G. Marr, B. M. Barnes, and B. B. Boyer), and NSF Grant NSF-0117104 (B. M. Barnes).

REFERENCES

1. Altschul SF, Gish W, Miller W, Myers EW, and Lipman DJ. Basic local alignment search tool. *J Mol Biol* 215: 403–410, 1990.

2. **Andrews MT, Squire TL, Bowen CM, and Rollins MB.** Low-temperature carbon utilization is regulated by novel gene activity in the heart of a hibernating mammal. *Proc Natl Acad Sci USA* 95: 8392–8397, 1998.
3. **Barnes BM.** Freeze avoidance in a mammal: body temperatures below 0°C in an Arctic hibernator. *Science* 244: 1593–1595, 1989.
4. **Bauer VW, Squire TL, Lowe ME, and Andrews MT.** Expression of a chimeric retroviral-lipase mRNA confers enhanced lipolysis in a hibernating mammal. *Am J Physiol Regul Integr Comp Physiol* 281: R1186–R1192, 2001.
5. **Boyer BB, Barnes BM, Kopecky J, Jacobsson A, and Hermanska J.** Molecular control of prehibernation brown fat growth in arctic ground squirrels. In: *Life in the Cold III: Ecological, Physiological and Molecular Mechanisms*, edited by Carey C, Florant GL, Wunder BA, and Horwitz B. Boulder, CO: Westview, 1993.
6. **Boyer BB and Barnes BM.** Molecular and metabolic aspects of mammalian hibernation. *Bioscience* 49: 713–724, 1999.
7. **Bradshaw AD, Graves DC, Motamed K, and Sage EH.** SPARC-null mice exhibit increased adiposity without significant differences in overall body weight. *Proc Natl Acad Sci USA* 100: 6045–6050, 2003.
8. **Brauch KM, Dhruv ND, Hanse EA, and Andrews MT.** Digital transcriptome analysis indicates adaptive mechanisms in the heart of a hibernating mammal. *Physiol Genomics* 23: 227–234, 2005.
9. **Buck CL and Barnes BM.** Effects of ambient temperature on metabolic rate, respiratory quotient, and torpor in an arctic hibernator. *Am J Physiol Regul Integr Comp Physiol* 279: R255–R262, 2000.
10. **Buzadzic B, Spasic M, Saicic ZS, Radojicic R, Petrovic VM, and Halliwell B.** Antioxidant defenses in the ground squirrel *Citellus citellus*. 2. The effect of hibernation. *Free Radic Biol Med* 9: 407–413, 1990.
11. **Cannon B and Nedergaard J.** Brown adipose tissue: function and physiological significance. *Physiol Rev* 84: 277–359, 2004.
12. **Carey HV, Andrews MT, and Martin SL.** Mammalian hibernation: cellular and molecular responses to depressed metabolism and low temperature. *Physiol Rev* 83: 1153–1181, 2003.
13. **Daikoku T, Shinohara Y, Shima A, Yamazaki N, and Terada H.** Dramatic enhancement of the specific expression of the heart-type fatty acid binding protein in rat brown adipose tissue by cold exposure. *FEBS Lett* 410: 383–386, 1997.
14. **Eddy SF, Morin P Jr, and Storey KB.** Cloning and expression of PPAR- γ and PGC-1 α from the hibernating ground squirrel, *Spermophilus tridecemlineatus*. *Mol Cell Biochem* 269: 175–182, 2005.
15. **Epperson LE and Martin SL.** Quantitative assessment of ground squirrel mRNA levels in multiple stages of hibernation. *Physiol Genomics* 10: 93–102, 2002.
16. **Epperson LE, Dahl TA, and Martin SL.** Quantitative analysis of liver protein expression during hibernation in the golden-mantled ground squirrel. *Mol Cell Proteomics* 3: 920–933, 2004.
17. **Fahlman A, Storey JM, and Storey KB.** Gene up-regulation in heart during mammalian hibernation. *Cryobiology* 40: 332–342, 2000.
18. **Frerichs KU, Smith CB, Brenner M, DeGracia DJ, Krause GS, Marrone L, Dever TE, Hallenbeck JM.** Suppression of protein synthesis in brain during hibernation involves inhibition of protein initiation and elongation. *Proc Natl Acad Sci USA* 95: 14511–14516, 1998.
19. **Hittel DS and Storey KB.** Differential expression of adipose- and heart-type fatty acid binding proteins in hibernating ground squirrels. *Biochim Biophys Acta* 1522: 238–243, 2001.
20. **Hittel DS and Storey KB.** Differential expression of mitochondria-encoded genes in a hibernating mammal. *J Exp Biol* 205: 1625–1631, 2002.
21. **Kari L, Loboda A, Nebozhyn M, Rook AH, Vonderheid EC, Nichols C, Virok D, Chang C, Horng WH, Johnston J, Wysocka M, Showe MK, and Showe LC.** Classification and prediction of survival in patients with the leukemic phase of cutaneous T-cell lymphoma. *J Exp Med* 197: 1477–1488, 2003.
22. **Knight JE, Narus EN, Martin SL, Jacobson A, Barnes BM, and Boyer BB.** mRNA stability and polysome loss in hibernating Arctic ground squirrels (*Spermophilus parryii*). *Mol Cell Biol* 20: 6374–6379, 2000.
23. **Long RA, Martin TJ, and Barnes BM.** Body temperature and activity patterns in free-living arctic ground squirrels. *J Mammal* 86: 312–322, 2005.
24. **Milner RE, Wang LC, and Trayhurn P.** Brown fat thermogenesis during hibernation and arousal in Richardson's ground squirrel. *Am J Physiol Regul Integr Comp Physiol* 256: R42–R48, 1989.
25. **Saitongdee P, Milner P, Becker DL, Knight GE, Burnstock G.** Increased connexin43 gap junction protein in hamster cardiomyocytes during cold acclimatization and hibernation. *Cardiovasc Res* 47: 108–115, 2000.
26. **Soukri A, Valverde F, Hafid N, Elkebbaj MS, and Serrano A.** Occurrence of a differential expression of the glyceraldehyde-3-phosphate dehydrogenase gene in muscle and liver from euthermic and induced hibernating jerboa (*Jaculus orientalis*). *Gene* 181: 139–145, 1996.
27. **Srere HK, Wang LCH, and Martin SL.** Central role for differential gene expression in mammalian hibernation. *Proc Natl Acad Sci USA* 89: 7119–7123, 1992.
28. **Tvrđik P, Kuzela S, and Houstek J.** Low translational efficiency of the F1-ATPase beta-subunit mRNA largely accounts for the decreased ATPase content in brown adipose tissue mitochondria. *FEBS Lett* 313: 23–26, 1992.
29. **Van Breukelen F and Martin SL.** Translational initiation is uncoupled from elongation at 18°C during mammalian hibernation. *Am J Physiol Regul Integr Comp Physiol* 281: R1374–R1379, 2001.
30. **Van Gelder RN, von Zastrow ME, Yool A, Dement AC, Barchas JD, and Eberwine EH.** Amplified RNA synthesized from limited quantities of heterogeneous cDNA. *Proc Natl Acad Sci USA* 87: 1663–1667, 1990.
31. **Williams DR, Epperson LE, Li W, Hughes MA, Taylor R, Rogers J, Martin SL, Cossins AR, and Gracey AY.** Seasonally hibernating phenotype assessed through transcript screening. *Physiol Genomics* 24: 13–22, 2005.
32. **Wilson BE, Deeb S, and Florant GL.** Seasonal changes in hormone-sensitive and lipoprotein lipase mRNA concentrations in marmot white adipose tissue. *Am J Physiol Regul Integr Comp Physiol* 262: R177–R181, 1992.
33. **Zeeberg BR, Feng W, Wang G, Wang MD, Fojo AT, Sunshine M, Narasimhan S, Kane DW, Reinhold WC, Lababidi S, Bussey KJ, Riss J, Barrett JC, and Weinstein JN.** GoMiner: a resource for biological interpretation of genomic and proteomic data. *Genome Biol* 4: R28, 2003.